Time domain simulation of torsional-axial and lateral vibration in drilling operation

B.M.Imani[1], S.G.Moosavi[2]
[1]Faculty of Engineering, Ferdowsi University of Mashhad, Mashhad, Iran
[2]Faculty of Engineering, Ferdowsi University of Mashhad

***Abstract*- Drilling process is one of the common traditional machining operations. Due to time inefficiency of the drilling process, it is considered as a critical operation that considerably affects the time of the entire machining process. Therefore, finding optimal conditions which result in increase in material removal rate (MRR) is of great importance. In order to increase cutting velocity, width of cut and feed, drilling system should be dynamically analyzed. Stability of the operation should also be investigated in different operational conditions. In this research a new force model has been proposed which are validated using experimental tests. Simulation of torsional-axial vibration is carried out using Bayly's vibration model. This model is based on the fact that when a twist drill "untwists", it extend in length. In other words, both twisting and axial deflection are coupled. Boundary conditions which are considered in simulation of lateral vibration are decoupled in to two parts so that they can mimic boundary conditions of the drilling process more realistically. Boundary conditions in start of drilling operation are considered to be clamped-free. They changed to clamped-pin conditions for the rest of operation when drill is completely engaged in the hole. Applying these boundary conditions, dynamic undeformed chip thickness is also determined. Simulation of lateral vibration is carried out using the proposed force model. Simulation results are verified by experiments.**

Keywords: Time domain simulation, dynamic undeformed chip thickness, lateral vibration, Edge force.

I. INTRODUCTION

One of the widely used approaches in stability analysis is time domain simulation, which allows a better insight into the dynamics of cutting. Also, the effect of basic nonlinearity can be taken into account and a more accurate estimation of cutting forces can be obtained [1]. In order to simulate drilling vibration, it is important to predict cutting force and vibrations of the system when boundary conditions for drilling vibration are applied. Simulation of drilling vibration has recently been studied by Roukema and Altintas[2]. They obtained cutting pressure for different widths of cut as well as different feeds for specific drill geometry while spindle speed was constant. They found a second and third order function describing cutting pressure in term of unformed chip thickness and a drill radius, respectively. Force model proposed by Roukema and Altintas can't use for different spindle speeds and drill with different radius. Mathematical model of the drill that used was a clamped-free beam with four degree of freedom (two degree for lateral and one for axial and one for torsional direction). Tooraj Arvajeh and Fathy Ismail [1, 3] used a specific drill, feed and spindle speed to determine cutting pressure for different widths of cut. They obtained cutting pressure along the cutting edge as a second order function of drill radius. Their force model did not include drill with different radius, spindle speed and feed. The mathematical model for lateral vibration that they used was a beam with clamped-pin boundary condition.

Empirical functions describing the drilling cutting force have been established for Al6061-T6 workpiece and HSS tool by R.F.Hamade, C.Y.Seif and F.Ismail [4]. This cutting force model uses the empirical cutting pressures which are represented in the form:

$$C_z = \frac{F_z}{bh} = a_1 h^{b_1} V^{c_1} (1 - \sin(\alpha))^{d_1} \quad (1)$$

$$C_t = \frac{F_t}{bh} = a_2 h^{b_2} V^{c_2} (1 - \sin(\alpha))^{d_2} \quad (2)$$

Where C_z and F_z are cutting pressures and cutting force in direction of drill axis respectively and C_t, F_t are cutting pressure and cutting force in tangential direction of the cutting edge respectively. h is undeformed chip thickness, V is linear velocity of cutting element, α is rake angle of cutting element and b is width of cut. Coefficients (a, b, c, d) are determined by drilling experiments. This force model can be used for prediction of cutting force with different feed, speed, rake angle and width of cut.

The development of torsional-axial vibration model by Bayly has been a major milestone in understanding chatter in machining using twist drills. Bayly's model is based on the fact that when a twist drill "untwists", it extends in length. In other words, both twisting and axial deflection are coupled [4]. Bayly considered the lumped mass model, depicted in Fig. 1, in which the torsional deflection, θ, creates the axial elongation, z.

According to Bayly, the equation of motion of the coupled torsional-axial mode can be written as:

$$m\ddot{z}(t) + c\dot{z}(t) + kz(t) = F_z(t) - (r\theta)F_t(t) \quad (3)$$

Where m, c and k are the mass, damping and stiffness; F_z and F_t are the dynamic parts of thrust and tangential force, respectively; and (rθ) represents the torsional "unwinding" of the drill cutting edge due to one unit of axial compression [5].

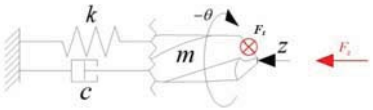

Fig. 1. Lumped model for torsional-axial vibration [5]

II. Force Model

Geometrical parameters (rake angle, inclined angle, helical angle and width of cut) vary greatly along the cutting edge of the twist drill therefore it is necessary to divide the cutting edge to smaller elements with constant value for these parameters. In R.F.Hamade, C.Y.Seif, F.Ismail [4] geometrical parameters were obtained only theoretically for each element (i.e. these parameters were not verified by experiment). In this paper we make a more realistic assumption by considering variation of rake angle inclined angle, helical angle and width of cut. Geometrical parameters of drill are function of its radius. These parameters are the same for drills with different radius and equal radius ratio (r/R) [6]. Therefore we propose the following equations for cutting pressures.

$$C_z = \frac{F_z}{bh} = a_1 h^{b_1} V^{c_1} (r/R)^{d_1} \quad (4)$$

$$C_t = \frac{F_t}{bh} = a_2 h^{b_2} V^{c_2} (r/R)^{d_2} \quad (5)$$

The proposed force model (4), (5) considers effects of geometrical parameters which are modeled by the term (r/R). r is radial distance of cutting element from drill axis and R is drill radius. Values of a_1-d_1 and a_2-d_2 in (4), (5) are obtained by experiments tests. In these equations geometrical parameters can be obtained by experiments although geometrical parameters used in (1) and (2) are obtained theoretically. Considering inherent errors of theoretical obtaining of these values, it can be stated that the proposed model can be have a more realistic prediction of cutting pressure.

A. Drilling tests

All drilling tests are performed using a lathe and the workpiece material is Al7075. In order to measure forces applied to the drill during drilling operation, a dynamometer (KISTLER type 9225B) along with Multichanel Charge Amplifier type 5070 and PC based data acquisition card with "MATLAB" for sampling are used. The dynamometer has capability of measuring forces in three orthogonal directions (Fx, Fy, Fz). In order to measure torque, a fixture is designed and manufactured which is shown in Fig. 2. The fixture has been calibrated before starting experiments.

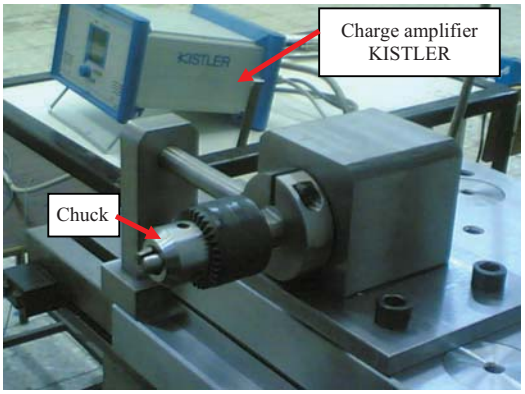

Fig. 2. Constructed fixture for holding and measuring torque

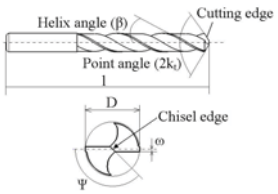

TABLE I
Drill Geometrical Parameters

Drill diameter (D)	10.5mm
Chisel thickness(2ω)	2mm
Point angle ($2k_t$)	118°
Helix angle (β)	29°
Chisel angle (ψ)	135°
Drill length (l)	280mm

B. Edge force

Measured axial forces and torques from experimental tests are sum of three components:

1- Cutting force and cutting torque (F_{zc} , M_c).
2- The force and torque attributed to ploughing at the main cutting edge (F_{ze},M_e).
3- Force and torque from rubbing action at the margin (friction between helical edge of the drill and workpiece) (F_{zm}, M_m).

$$F_z = F_{zc} + F_{ze} + F_{zm} \quad (6)$$

$$M = M_c + M_e + M_m \quad (7)$$

Where the subscripts c, e and m stand for cutting, edge, and margin respectively [4].

In order to obtain main cutting edge and margin contribution for axial force and torque we follow this procedure. First, we approximate axial forces and torques measured for different feed and specific predrilled with line. Next, the by extrapolating the obtained line for feed=0 mm/rev the main cutting edge and margin contributions to axial force and torque for specific predrilled are determined.

We applied R.F.Hamade method [3] by using measured cutting forces and torque to determined coefficients a, b and c in (4) and (5). In order to determine d_1 and d_2, cutting forces and torque are measured during drilling operation with different diameter of predrilled and constant feed and spindle speed. The value of axial force and torque for two specific predrilled diameters are subtracted and divided by width of cut between two predrilled diameters. For example we measure axial cutting force for 3 and 5 mm predrilled (width

of cut is 2mm and position of element is 4mm from the center of drill). Therefore, radius ratio of element (r/R) is calculated (4/10.5). The differential axial force is calculated by subtracting the value measured at 5 mm predrilled from that of 3 mm predrilled. Next, this value is divided by 2 mm (element width of cut). This value is plotted versus ratio of (r/R) for this element (4/10.5). The same procedure is followed for torque. These values can be obtained for different ratios of (r/R) from different predrilled workpieces. Fig. 4 shows the effect of geometrical parameters on axial cutting force and torque with spindle speed 1000 rpm. For spindle speeds of 250, 500, 710 and 1400 rpm, experiments are performed and coefficients a, b, c and d are obtained and listed in Table 2.

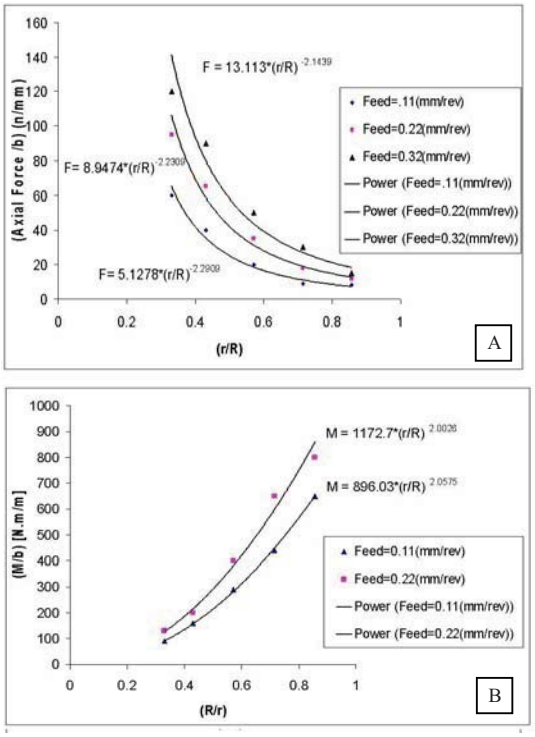

Fig. 4. Effect of geometrical parameters on (A) axial cutting force (B) cutting torque

TABLE 2
COEFFICIENTS FOR CUTTING PRESSURE DISTRIBUTION PER (4) AND (5)

C_z	a_1	b_1	c_1	d_1
	130	**-0.3**	**-0.13**	**-2.2**
C_t	a_2	b_2	c_2	d_2
	7.5	**-0.05**	**-0.12**	**2**

The difference between measured forces in experimental test and predicted forces by using new force model is shown in Fig. 5.

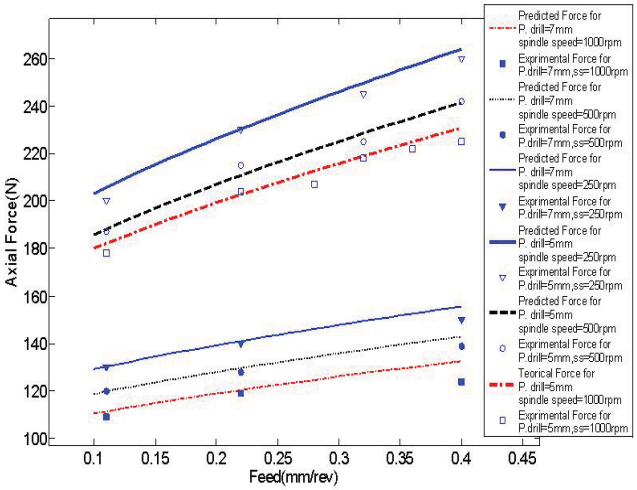

Fig. 5. Comparison of measured forces in experimental tests with predicted forces

III. DYNAMIC UNDEFORMED CHIP THICKNESS

Mainly two types of boundary conditions have been used by different researchers for mathematical modeling of drilling vibration [1, 2]. Boundary conditions in real drilling operation have two stages: Boundary conditions at the start of drilling operation which considered to be clamped-free. Afterwards, boundary condition is changed to clamped-pin for the rest of operation, when drill is completely engaged in the hole. Definition of undeformed chip thickness depends on boundary conditions of drilling operation. In the following, dynamic un-deformed chip thickness for clamped-free and clamped-pin boundary condition is defined.

A. Dynamic undeformed chip thickness with clamped-free boundary condition

Lateral motion of drill tip in clamped-free boundary condition is shown in Fig. 6. Chip thickness on each edge of drill with clamped-free boundary condition depends on:

1- x(t): drill radial run out defined as the deviation from the spindle axis in the direction of the cutting edge.
2- h_p: difference in edge height called axial run out.
3- e : edge angle error.
4- z(t): axial vibration.
5- (h=f×sin(k_t)/2): feed.

Therefore, the un-deformed chip thickness for each edge of drill with clamped-free boundary condition can be express as:

$$h_{d1}(t,r) = h - (z(t) - z(t-\tau)) \times \sin(k_t) + (x(t) - x(t-\tau)) \times \cos(k_t) + h_p + (r/\sin(k_t)) \times \tan(e)$$
$$h_{d2}(t,r) = h - (z(t) - z(t-\tau)) \times \sin(k_t) - (x(t) - x(t-\tau)) \times \cos(k_t) - (r/\sin(k_t)) \times \tan(e) \quad (8)$$

Where $2k_t$ is the tip angle of drill, h is chip thickness equal to (f/2)×sin(k_t) and z(t) is axial tool tip deflection. h_{d1} and h_{d2} are dynamic chip thickness for edge1 and edge 2, respectively.

Unequal chip thicknesses on two edges of drill (h_{d1} isn't equal to h_{d2}) cause lateral forces in drilling operation. In other

words, balanced chip thicknesses on two edges generate only axial force and torque. Unlike unequal chip thickness, balanced chip thickness doesn't create lateral forces.

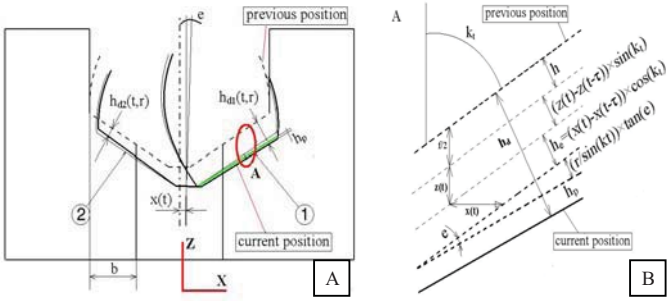

Fig. 6. (A) Variation of chip thickness for each cutting edge of drill with clamped- free B.C.[1] (B) zoomed area A in Fig. 6(A)

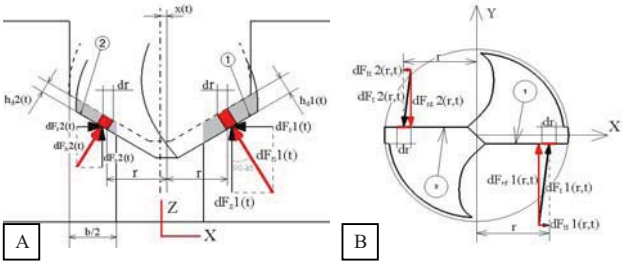

Fig. 7. Elemental force acting on the cutting edges of a two- fluted drill shown in (A) xz plane (B) xy plane

Differential cutting force components for drill with clamped-free B.C. are shown in Fig. 7. The dynamometer and fixture setup can measure torque (tangential force $F_t(t,r)$ can be calculated by dividing torque to element distance from the drill center) and axial force, $F_z(t)$. $F_z(t)$ is vertical component of normal force, $F_n(t)$. Horizontal component of normal force, $F_r(t)$ is shown in (Fig. 7A). Tangential component of $F_t(t)$ along the cutting edge, $F_{tt}(t)$ and its normal component, $F_{nt}(t)$ is shown in Fig. 7(B). Therefore torque and force components can be written as.

$$dF_x(t,r) = (dF_r 2(t,r) - dF_r 1(t,r)) - (dF_{tt} 2(t,r) - dF_{tt} 1(t,r)) \times \sin(k_t) \quad (9)$$

$$dF_y(t,r) = dF_{nt} 1(t,r) - dF_{nt} 2(t,r) \quad (10)$$

$$dF_z(t,r) = dF_z 1(t,r) + dF_z 2(t,r) + (dF_{tt} 1(t,r) + dF_{tt} 2(t,r)) \times \cos(k_t) \quad (11)$$

$$dM_{oz}(t,r) = r \times dF_t 1(t) + r \times dF_t 2(t) \quad (12)$$

Where,

$$\begin{aligned} dF_r(t,r) &= dF_z(t,r) \times \cot(k_t) \\ dF_{tt}(t,r) &= dF_t(t,r) \times \sin(i) \\ dF_{nt}(t,r) &= dF_t(t,r) \times \cos(i) \end{aligned} \quad (13)$$

Substituting (4) and (5) in to (13) and substituting (13) and (8) in to (9), (10), (11) and (12) elemental force components can be determined. The total cutting force components are evaluated by summation of elemental forces distributed along the cutting edges. Therefore components of cutting force can be determined as:

$$\begin{bmatrix} F_x(t) \\ F_y(t) \\ F_z(t) \\ F_t(t) \end{bmatrix} = \begin{bmatrix} \sum dF_x(t,r) \\ \sum dF_y(t,r) \\ \sum dF_z(t,r) \\ \sum dM_{oz}(t,r)/r \end{bmatrix} \quad (14)$$

B. Dynamic undeformed chip thickness with clamped-pin B.C.

Fig8 shows the drill rotated about its tip in clamped-pin B.C.

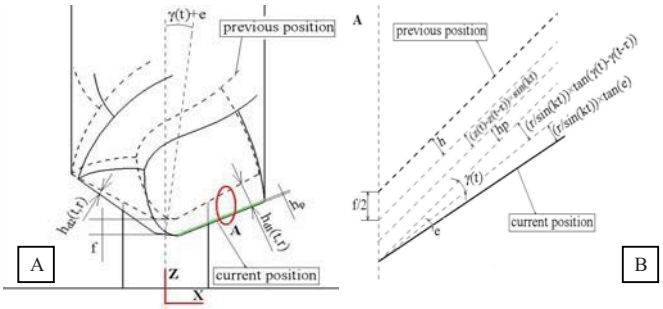

Fig. 8. (A)Variation of chip thickness in clamped-pin B.C. (B) zoomed area A in Fig. 8 (A)

Chip thickness on each edge of drill with clamped-pin boundary condition consists of:

1- γ(t):Drill rotation angle about drill tip.
2- h_p :The difference in edge height is called axial run out.
3- e :Edge angle error.
4- z(t):Axial vibration.
5- (h=f×sin (k_t)/2): Feed.

Undeformed chip thickness for each edge of drill with clamped-pin boundary condition can be written as:

$$\begin{aligned} h_d 1(t,r) &= h - (z(t) - z(t-\tau)) \times \sin(kt) + (r/\sin(kt)) \times \tan(\gamma(t) - \gamma(t-\tau)) \\ &+ h_p + (r/\sin(kt)) \times \tan(e) \\ h_d 2(t,r) &= h - (z(t) - z(t-\tau)) \times \sin(kt) - (r/\sin(kt)) \times \tan(\gamma(t) - \gamma(t-\tau)) \\ &- (r/\sin(kt)) \times \tan(e) \end{aligned} \quad (15)$$

In order to simulate drilling vibration with clamped-pin boundary condition, drill is assumed as a clamped-pinned beam whose mass is lumped at middle at z=l/2 as shown in Fig. 9 [1].

As can be seen in the Fig. 9, when the drill deflects in the X-direction or the Y-direction, the drill tip rotates about the Y-axis or the X-axis respectively. The rotation of the cutting edges causes a variation in cutting forces between the cutting edges which consequently creates a variation in moments of the cutting forces about the tip of drill in all directions; around X, Mx, around Y, My and round Z, Mz.

Cutting forces components for drill with clamped-pin boundary condition are shown in Fig. 10. Moments of cutting forces about X, Y and Z axis can be written as:

$$\begin{aligned} dMx(t,r) &= dF_{nt} 1(t,r) \times r \times \cot(k_t + \gamma(t)) - dF_{nt} 2(t) \times r \times \cot(k_t - \gamma(t)) \\ dMy(t,r) &= (dF_z 2(t,r) - dF_z 1(t,r) + dF_{tt} 1(t,r) \times \cos(k_t + \gamma(t)) - dF_{tt} 2(t,r) \times \\ &\cos(k_t - \gamma(t))) \times r + (dF_r 2(t,r) - dF_{tt} 2(t) \times \sin(k_t - \gamma(t))) \times r \times \cot(k_t - \gamma(t)) - \\ &(dF_r 1(t,r) - dF_{tt} 1(t,r) \times \sin(k_t + \gamma(t))) \times r \times \cot(k_t + \gamma(t)) \end{aligned} \quad (16\text{–}17)$$

$$dM_{oz}(t,r) = r \times dF_t 1(t) + r \times dF_t 2(t) \quad (18)$$

[1] . B.C. : boundary condition

Where dF_{nt}, dF_{tt} and dF_r are obtained by using (13) and axial force, F_z is obtained from:

$$dF_z(t,r) = dF_z1(t,r) + dF_z2(t,r) + (dF_{tt}1(t,r) + dF_{tt}2(t,r)) \times \cos(k_t) \quad (19)$$

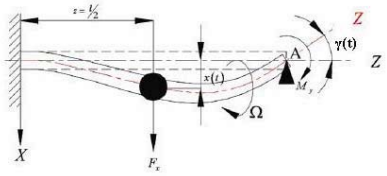

Fig. 9. Lumped mass model of drill for lateral vibration [1]

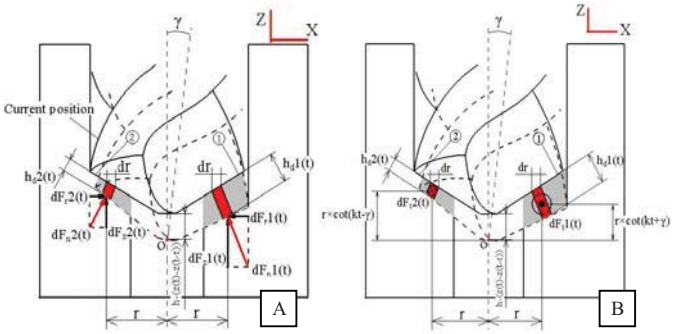

Fig. 10. Cutting force components (A) axial force (B) tangential force

Since the drill is assumed as a lumped mass at the middle, z=l/2, the moments about point A (Fig. 9) around X-axis, Mx and around Y-axis, My, is replaced by forces F_y and F_x, according to [1]:

$$F_x = -\frac{My}{l/2} \quad (20)$$

$$F_y = \frac{Mx}{l/2} \quad (21)$$

Substituting (4) and (5) in to (13) and substituting (13) and (15) in to (16), (17), (18) moment of cutting forces about X, Y and Z axis are determined. Then by using (20), (21) and (19) components of cutting force in X, Y, Z directions can be found. The total cutting forces are evaluated by summation of elemental forces distributed along the cutting edges (14).

IV. Dynamic Parameters Of Drill

Cutting and dynamic system parameters are needed for time domain simulation of cutting process. The cutting parameters are obtained using cutting force model, and dynamic parameters are obtained using finite element model in conjunction with the impact modal testing. The natural frequencies in different mode shapes with different boundary conditions are obtained from finite element method. These values are next compared with the values obtained from modal testing. Damping ratios are measured experimentally using modal testing. The obtained dynamic parameters for the drill with geometrical shown in table1, is listed in table3.

V. Time Domain Simulation

Time domain simulations are carried out by using Bayly's model, Fig. 1 for torsional-axial vibration and Ismail model, Fig. 9 for lateral vibration. Equations of motion used in simulation can be expressed as follows:

$$M\begin{bmatrix}\ddot{x}(t)\\ \ddot{y}(t)\\ \ddot{z}(t)\end{bmatrix} + C\begin{bmatrix}\dot{x}(t)\\ \dot{y}(t)\\ \dot{z}(t)\end{bmatrix} + K\begin{bmatrix}x(t)\\ y(t)\\ z(t)\end{bmatrix} = \begin{bmatrix}F_x(t)\\ F_y(t)\\ F_z(t) - (-r\theta)\times F_t(t)\end{bmatrix} \quad (22)$$

Where M, C, K contain the mass, damping and stiffness, respectively. x(t) and y(t) are the deflections of the middle of the drill and z(t) is the axial elongation of the drill tip. The right hand side of equation shows dynamic forces acting on the drill obtained by (14). Based on boundary condition of the drill (9), (10), (11) and (12) for clamped-free B.C or (18), (19), (20) and (21) for clamped-pin B.C, dynamic forces will be obtained. Results of measured axial and lateral forces in experimental drilling test and FFT of axial and lateral forces data are shown in Fig. 11. In this experiment, spindle speed is 1000rpm, predrilled is 5mm and feed is 0.11 mm/rev.

TABE III
Dynamic Parameters

Boundary condition	Clamped-Pin	Clamped-free
natural Frequency in axial direction	2600[Hz]	2600[Hz]
natural Frequency in lateral direction	475[Hz]	132 [Hz]
Damping ratio	0.006	0.008

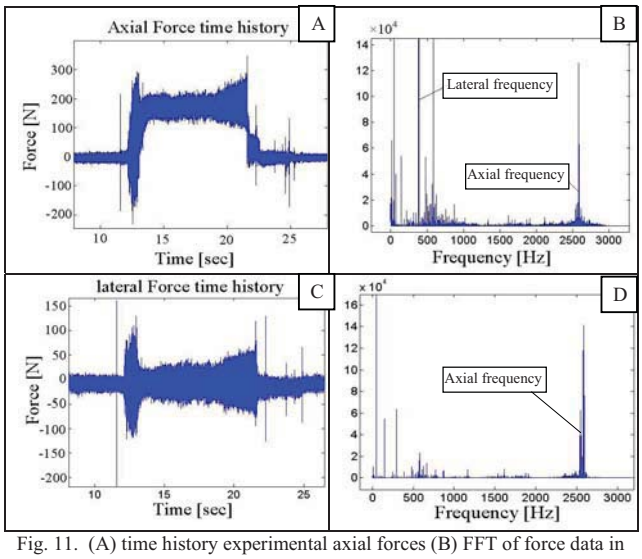

Fig. 11. (A) time history experimental axial forces (B) FFT of force data in axial direction (C) Time history Experimental lateral forces (D) FFT of force data in lateral direction

Fig. 11(A) shows the time trace of axial force. Since axial vibrations amplitude grows (at time 15 to 22 sec), unstability occurred at axial mode. Fig. 11 (B) shows FFT of force data in axial direction, as can be seen two strong peaks at the frequency around 450 Hz (lateral frequency) and at the

frequency around 2600 Hz (axial frequency). Fig. 11(C) shows the time trace of lateral force. Since amplitude of vibrations in lateral direction grows therefore at lateral mode is unstable. Fig. 11(D) shows FFT of force data in lateral direction, as can be seen a large peak at the frequency around 2600 Hz (axial frequency). It should be noted that lateral frequency appear in axial vibration and axial frequency appear in lateral vibration, Fig. 11(B) and Fig. 11(D).

Simulations of axial and lateral vibration are carried out by using the proposed force model. To solve the equations of motion, (22) fourth order Rung-Kutta method is used. Simulation of axial force time history is shown in Fig. 12. Time domain simulation, Fig. 12(A) and Fig. 12(B) shows unstability in axial direction for spindle speed 1000 rpm, predrilled 5mm and feed 0.11 mm/rev. FFT of simulated axial force data, Fig. 12(B) shows two peaks at the frequency around 450 Hz and frequency around 2700Hz. The simulation results of axial force with new force model and dynamic undeformed chip thickness in Fig. 12 are in close agreement with experimental results Fig. 11.

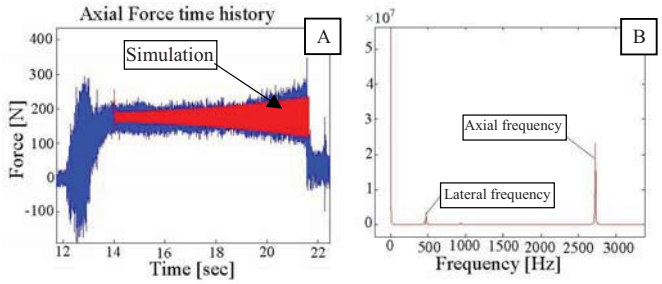

Fig. 12. (A) Result of time domain simulation of axial force and comparison with experimental result for spindle speed 1000 rpm, predrilled 5mm and feed 0.11 mm/rev (B) Frequency excited of simulated axial force

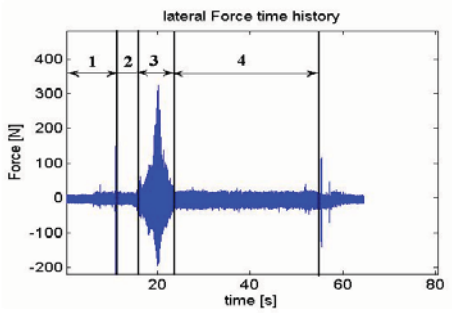

Fig. 13. Different regions in lateral vibration

Because of presence of term F_{tt} in (11) and (19) lateral frequency is appeared in axial vibration, Fig. 12(B).

For simulation of lateral force, different regions vibration mentioned in section (III) should be considered. Different regions in lateral vibration for spindle speed 500rpm, predrilled 5mm and feed 0.05 mm/rev are shown in Fig. 13. As can be seen in Fig. 13 four different regions: in first region drill has not yet engaged with the workpiece (region 1 in Fig. 13). Second region drill is beginning to engage with the workpiece (region 2 in Fig. 13). In Third region drill is engaged with the workpiece and lateral vibration is unstable, boundary condition in this region is clamped-free (region 3 in Fig. 13). Fourth region drill completely engaged with workpiece and lateral vibration is stable .Boundary condition in fourth region is clamped-pin (region 4 in Fig. 13). Therefore different boundary conditions for simulations of third and fourth regions are importance. Simulation results for lateral vibration with clamped-pin and clamped- free boundary condition are shown in Fig. 14. As can be seen in Fig. 14 lateral vibration is unstable in clamped-free boundary condition and is stabile in clamped-pin boundary condition with the same spindle speed, predrilled and feed. These simulation results agree with the third and fourth region in experimental test, Fig. 13.

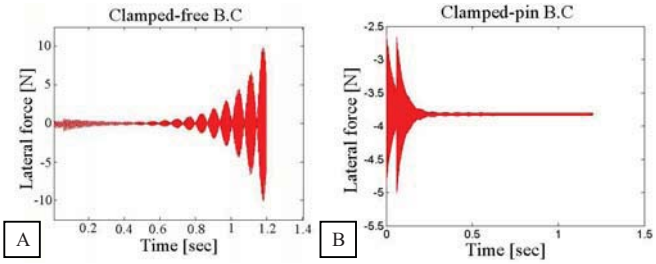

Fig. 14. Time domain simulation with (A) clamped-free (B) clamped-pin boundary condition for spindle speed 500 rpm, predrilled 5mm and feed 0.05 mm/rev

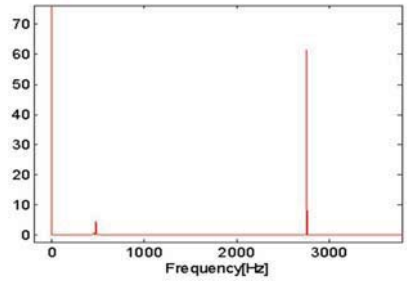

Fig. 15. Frequency content of lateral force simulation

Simulation result of lateral force with clamped- pin boundary condition for spindle speed 1000 rpm, predrilled 5 mm and feed 0.11 mm/rev is shown in Fig. 15. Fig. 15 shows unstability in lateral vibration that is verified with experimental test, Fig 11(D). Because of presence of term F_z in (9) and (17) axial frequency is appeared in lateral vibration Fig. 15.

V. CONCLUSIONS

In this paper we proposed a new force model base on experimental drilling tests. Effect of linear cutting velocity, feed and geometrical parameters are taken in to account in proposed force model. Coefficients of cutting pressures in new force model are completely determined from experimental drilling tests without using theoretical equations. In the proposed force model effect of geometrical parameters

are modeled by the term (r/R). Although in (1) and (2) geometrical parameters are modeled by the term rake angle (α) which obtained theoretically. Inherent errors consider theoretical obtaining of this value. Results of predicted forces by using new force model were in close agreement with forces measured from experimental drilling tests with specific drill geometry. The proposed force model can be verified for drill with different diameters and compared with experimental tests. This model can also be tested for high speed drilling.

In this paper an equation for dynamic undeformed chip thickness is presented based on a more precise model for boundary conditions of the drill. Boundary conditions at the beginning of drilling operation are modeled as clamped-free. Next, boundary conditions changed to clamped-pin when drill is completely engaged in workpiece. For each boundary condition, components of cutting force were determined. Simulation of torsional and axial vibration carried out by using Bayly's model. Result of simulation is verified by experimental test. The reason of appearance of lateral frequency in axial vibration is explained by simulation using the proposed force model. (Presence of component of tangential force along the cutting edge in axial direction.) The existence of different stages in drilling vibration is justified by considering different boundary conditions for each stage. Results of lateral force simulation based on different boundary conditions in drilling operation are verified by experimental results.

REFERENCES

[1] Tooraj Arvajeh and Fathy Ismail,"Machining stability in high-speed drilling-Part 1:Modeling vibration stability in bending", International Journal of Machine Tools & Manufacture 46(2006) 1563-1572.

[2] Jochem C.Roukema,Yusuf Altintas, "Generalized modeling of drilling vibrations, Part I: Time domain model of drilling kinematics, dynamics and hole formation "International Journal of Machine Tools & Manufacture,2006

[3] Tooraj Arvajeh, Fathy Ismail,"Machining stability in high speed drilling-part 2: Time domain simulation of a bending-torsional model and experimental validations", International Journal of Machine Tool & Manufacture, 46 (2006) 1573-1581.

[4] R. Hamade, C.Y. Seif, F. Ismail,"Using drilling experiments to extract specific cutting force coefficients", International Journal of Machine Tools and Manufacture, 46 (2006) 387-396.

[5] Toraj Arvajeh and Fathy Ismail," Stability lobes of Twist drills including profiles of geometrical and cutting parameters along the cutting edge "Department of Mechanical Engineering, University of Waterloo, CIRP 2005

[6] V.Chandrasekharan, S.G. kapoor, R. E. DeVor "A Mechanistic Approach to predicting the Cutting Forces in Drilling: With Application to Fiber-Reinforced Composite Materials.